

String models of glueballs and the spectrum of $SU(N)$ gauge theories in 2+1 dimensions

Robert W. Johnson and Michael J. Teper

*Theoretical Physics, University of Oxford, 1 Keble Road,
Oxford OX1 3NP, UK*

Abstract.

The spectrum of glueballs in 2+1 dimensions is calculated within an extended class of Isgur-Paton flux tube models and is compared to lattice calculations of the low-lying $SU(N \geq 2)$ glueball mass spectrum. Our modifications of the model include a string curvature term and different ways of dealing with the flux tube width. We find that the generic model is remarkably successful at reproducing the positive charge conjugation, $C = +$, sector of the spectrum. The only large (and robust) discrepancy involves the 0^{-+} state. This raises the interesting possibility that the lattice spin identification is mistaken and that this state is in fact 4^{-+} . In addition, the Isgur-Paton model does not incorporate any mechanism for splitting $C = +$ from $C = -$ (in contrast to the case in 3+1 dimensions), while the ‘observed’ spectrum shows a substantial splitting. We explore several modifications of the model in an attempt to incorporate this physics in a natural way. At the qualitative level we find that this constrains our choice to the picture in which the $C = \pm$ splitting is driven by mixing with new states built on closed loops of adjoint flux. However a detailed numerical comparison suggests that a model incorporating an additional direct mixing between loops of opposite orientation is likely to work better; and that, in any case, a non-zero curvature term will be required. We also point out that a characteristic of any string model of glueballs is that the $SU(N \rightarrow \infty)$ mass spectrum will consist of multiple towers of states that are scaled up copies of each other. To test this will require a lattice mass spectrum that extends to somewhat larger masses than currently available.

1 Introduction

While it is now possible to calculate the spectrum of continuum non-Abelian gauge theories with some precision, using standard lattice Monte Carlo techniques [1, 2, 3], we know little about the structure of these glueballs. This is to be contrasted with states containing quarks where, at least for the low-lying spectrum, the quark model provides a remarkably successful semi-quantitative model framework for understanding the structure of mesons and baryons. (Apart from the interesting cases of scalar mesons and pseudoscalar flavour-singlet mesons.)

Having a model is desirable for many reasons, even if one can calculate the actual masses by other means. A simple model provides an intuitive understanding of the dynamics which allows one to estimate what occurs in a wide variety of physical situations. It can provide the basis for unexpected generalisations.

The glueballs of the SU(3) non-Abelian gauge theory in 3+1 dimensions are particularly important because the presence of such extra non-quarkonium states in the spectrum of QCD (and in the experimental spectrum) would provide a direct reflection of the gauge fields in the theory. Understanding just how they do so (mixing, decays etc.) would be made easier if we understood something about their structure. Unfortunately, beyond providing some information about glueball sizes, lattice Monte Carlo calculations have as yet given us little insight into their structure. Such calculations involve connected correlators of several operators and while they are simple in principle it is, in practice, much harder to achieve sufficient statistical accuracy than in the corresponding mass calculations.

An alternative way to learn about the structure of glueballs is through a reliable model – just as the quark model provides us with useful information on the structure of the low-lying mesons and baryons. To establish whether a glueball model is ‘reliable’ one can compare the spectrum it predicts to the known spectrum (as calculated from the lattice). This is the approach we follow here. There are two obvious models that one might try: constituent gluon models, such as gluon potential or bag models [4, 5], and flux tube (string) models [6]. In this paper we shall confine ourselves to a study of the latter.

Models try to isolate the essential physics and neglect everything else; thus they necessarily involve approximations. So one does not expect precise agreement with the known spectrum. If we are only looking for semi-quantitative or even qualitative agreement, it is important to test the model in as many relevant contexts as possible. One fact we can usefully use here is that string models (and indeed bag models) can be equally motivated in any gauge theory that has linear confinement and hence string-like flux tubes. This suggests that it would be useful to test this model not only in 3+1 dimensions [7] but also in 2+1 dimensions where non-Abelian gauge theories appear to be linearly confining and detailed mass spectra are available [3]. This is what we shall do in this paper. (We remark that recent improvements in the lattice calculation of the D=3+1 SU(3) spectrum [2] warrant a complete update of the study in [7].)

In the next section we briefly review the Isgur-Paton flux tube model for glueballs [6] and describe the qualitative features of the mass spectrum that it predicts for $SU(N)$ gauge theories in $D=2+1$. We compare this spectrum with the ‘true’ spectrum as calculated on the lattice, [3], which, for the reader’s convenience, we summarise in Table 1 borrowed from [3]. We point out where the main discrepancies and difficulties lie and we point out some compelling generalisations of the model. In the subsequent section we address a major such difficulty: how to incorporate an acceptable $C = \pm$ splitting into the model. We finish with a summary of our results.

This work builds upon the earlier work of [7] where the Isgur-Paton model was compared to the $SU(2)$ spectrum in both $2+1$ and $3+1$ dimensions. In $SU(2)$ there is no $C = -$ sector and any mixing/decay corrections will be maximal. However at the time there were no other $D=2+1$ spectra to compare against. That has changed and a much more complete analysis is now possible. We also draw the reader’s attention to an analysis of the $Z(2)$ gauge theory using the flux tube model [8]. Finally we remark that a summary of some of our preliminary results has appeared elsewhere [9], and a much more detailed exposition will appear in [10].

2 The standard flux tube model of glueballs

Consider a quark and an antiquark sufficiently far apart. In a linearly confining theory, they will be joined by a flux tube which contributes an energy that is approximately proportional to its length. One can attempt to use such states as the basis for a flux tube model of quarkonia. What about glueballs? The corresponding model for these would be one based on a loop of fundamental colour flux that closes on itself. This is a colour singlet object and it contains no quarks. If we neglect the thickness of this flux tube then what we have is a closed string and the glueball mass spectrum is obtained by finding the energy eigenstates of the quantised string. This is the starting point for the Isgur-Paton model [6] which we shall now briefly describe.

2.1 The Isgur-Paton flux tube model

We start with a closed string of colour flux in the form of a circle of radius ρ . Suppose it possesses a bare string tension σ_b and hence a bare energy

$$E_b = 2\pi\sigma_b\rho. \quad (1)$$

Consider now fluctuations about this circle. These can be decomposed as

$$\rho(\phi) = \rho + \sum_m (\alpha_m \sin m\phi + \beta_m \cos m\phi) \quad (2)$$

using radial and angular coordinates. If we quantise these fluctuations then we obtain states containing various numbers of phonons of various frequencies. That is to say the

state can be characterised by occupation numbers n_m^\pm , where the \pm labels the helicity of the mode, m/ρ is the frequency of the mode and $\pm m$ its contribution to the angular momentum. So such modes will contribute

$$J = \sum_{m=2} m(n_m^+ - n_m^-) \quad (3)$$

to the angular momentum of the state. Indeed since the underlying circular loop is rotationally invariant, this will be the total angular momentum of the state. The phonons will also contribute an energy

$$E_{\text{phonons}} \equiv \frac{M}{\rho} = \frac{1}{\rho} \sum_{m=2} m(n_m^+ + n_m^-) \quad (4)$$

to the total energy of the state. Note that the above sums begin with the $m = 2$ mode. The $m = 1$ mode is excluded in the model [6] because infinitesimal $m = 1$ fluctuations are the same as infinitesimal translations of the circle.

As usual when one quantises over modes of all frequencies there is a divergent contribution to the vacuum energy. In our case this has the form

$$\delta E = c\rho - \frac{13}{12\rho} + \dots \quad (5)$$

where c diverges as one removes whatever short distance cut-off one is using. This divergent piece can be absorbed into the renormalised string tension, $\sigma = \sigma_b + c/2\pi$. The second term is a string Casimir energy. It is universal for bosonic strings and, in the case where the strings end on static quarks, is called the Lüscher term [11]. In the present case the string has periodic rather than fixed boundary conditions, just as in calculations involving Polyakov loops [12], but the coefficient differs due to the exclusion of the $m = 1$ mode. Putting all this together we can write the energy of the string plus its modes as

$$E_s = 2\pi\rho\sigma - \frac{13}{12\rho} + \frac{1}{\rho} \sum_{m=2} m(n_m^+ + n_m^-) \quad (6)$$

However, we know that what we have is not really a one-dimensional string but rather a flux tube whose width will be $\sim 1/\sqrt{\sigma}$. For the low-lying states of interest to us we expect $\rho \sim 1/\sqrt{\sigma}$ and so one might expect the simple harmonic fluctuations of the flux tube to be somehow suppressed. This is incorporated within the Isgur-Paton model [6] by multiplying the contribution of the phonons to the energy (including that of the vacuum) by a heuristic suppression factor that rapidly approaches unity as ρ increases. This leads to a final string energy

$$E_s^M(\rho) = 2\pi\rho\sigma + \frac{M - \gamma}{\rho} F(\rho) \quad (7)$$

where $\gamma = -13/12$, M is defined in eqn(4) and $F(\rho)$ is the factor that suppresses the string excitations at small ρ . In the original model this was chosen to be

$$F(\rho) = 1 - e^{-f\rho} \quad (8)$$

where f is a parameter which we would expect to be $O(\sqrt{\sigma})$. This form is reasonable but somewhat arbitrary; one might ask, for example, why the string energy, $2\pi\rho\sigma$, is not modified at small ρ as well.

So much for the fluctuations about the circle. What of the radial fluctuations of the whole circle? In the Isgur-Paton model one identifies the conjugate momentum for the string and writes a Schrodinger equation in the radial coordinate ρ :

$$\left\{ \frac{-9}{16\pi\sigma} \frac{d^2}{d\xi^2} + E_s^M(\xi^{2/3}) \right\} \psi(\xi) = E\psi(\xi) \quad (9)$$

where $\xi = \rho^{3/2}$ turns out to be the natural variable to use here. This formalism assumes that the phonon modes are ‘fast’ compared to the collective radial modes and that they can therefore be treated as providing an effective potential for these latter modes. Clearly such an ‘adiabatic’ assumption is at best approximate: the model has only one scale, $\sqrt{\sigma}$, and so there is no reason for the phonon fluctuations to be *much* faster than the collective radial fluctuations for the low-lying part of the spectrum that will interest us. (Indeed if one calculates [7] the low-lying spectrum one finds that the energy splitting associated with an increment in the phonon number is of the same order as the splitting associated with an increment in the radial quantum number. This suggests that the division into fast and slow modes is a crude approximation at best.)

If we were in 3+1 rather than in 2+1 dimensions, the above description of the model would change as follows. First, rotations of the flux-loop around a diameter provide an additional source of angular momentum, and eqn(9) acquires a corresponding angular momentum term. In addition there are extra phonons arising from fluctuations of the loop normal to its plane. This doubling of modes leads to a doubling of the value of the string Casimir energy in eqn(6).

2.2 The spectrum of the model

To obtain the spectrum of the model one can solve eqn(9) numerically, as described in the Appendix, and then compare it in detail to the lattice spectrum [3], as summarised in Table 1. However the qualitative features of the model spectrum, such as degeneracies under parity and charge conjugation and much of the level-ordering, are robust against minor changes in the model and, as we shall now see, are easy to deduce.

2.2.1 qualitative features

First we recall that for $SU(N \geq 3)$ a string (or tube) of fundamental flux has a direction, so a circular string will have one of two orientations. These we label by L and R . Under charge conjugation, \mathcal{C} , the orientation of the glue loop is reversed, $L \leftrightarrow R$, and this is the only action of \mathcal{C} . Since there is no mixing between the L and R loops in the model, each of these loops will provide the basis for an identical spectrum. That is to say, states of $C = \pm$ (corresponding to the linear combinations $L \pm R$) will be degenerate. This is not the case in the observed spectrum (see Table1) and how to introduce a $C = \pm$ splitting, in a natural way, will be one of our main concerns in this paper. Note that this problem does not arise for $SU(2)$, the case considered in [7], since in that case the loop has no orientation.

Our second observation is that the model has a single mass scale $\sqrt{\sigma}$ (apart from the short-distance fudge factor f) and so all masses arise as simple multiples of this scale: double $\sqrt{\sigma}$ and you double all the masses. In addition we expect $f \propto \sqrt{\sigma}$ since it has to do with the width of the fluxtube, so it does not really provide an independent scale. So from now on we shall express everything explicitly in units of $\sqrt{\sigma}$ except where it turns out to be convenient to do otherwise.

In addition to having one scale, the model has no explicit dependence on any parameters, such as g^2 or N . Thus It predicts exactly the same spectrum for all $SU(N)$ groups. (Apart from the lack of a $C = -$ spectrum for $SU(2)$.) As a first approximation this is not, in fact, so bad: one finds (see Table1) [3] that the low-lying $SU(N \geq 2)$ mass spectrum is equal to that of the $SU(N = \infty)$ theory up to only a modest $O(1/N^2)$ correction.

Since the model incorporates no $C = \pm$ splitting, it is tempting to restrict its use to $SU(2)$. This would however be to merely hide the problem. In fact a much better argument can be made for applying the model, suitably extended, to $SU(N = \infty)$. The basic model does not incorporate finite decay widths (and mixings) which exist at finite N and which will alter the mass spectrum. It is only for $N = \infty$ that these effects disappear in the theory [13].

As a final general remark we note that under parity, \mathcal{P} , the loop orientation is flipped $L \leftrightarrow R$ and phonons have their helicity flipped, $n_m^+ \leftrightarrow n_m^- \ \forall m$ and so $J \rightarrow -J$. This implies that for $J \neq 0$ the spectrum is parity doubled. This is in fact a general, model-independent feature of the mass spectrum in 2 space dimensions which is reproduced, as it should be, by the lattice calculations [3].

The fact that $L \leftrightarrow R$ under both \mathcal{P} and \mathcal{C} , leads to the following specific degeneracies. Labelling states by L or R and $\{n_m^\pm\}$ it is straightforward to see that 0^{++} states are degenerate with 0^{--} and 0^{-+} with 0^{+-} . For $J \neq 0$ we find that all the four states with $C = \pm$ and $P = \pm$ are degenerate. This is also the case for $J = 0$ states in which the left and right helicity phonon content is not identical. As we have already remarked, while the parity doubling for $J \neq 0$ must remain exact, the $C = \pm$ degeneracies are broken in the observed spectrum, and one of our tasks is to see if there is a natural

extension of the model that will accommodate the observed breaking.

We can also say something about the mass spectrum by noting what is the minimal phonon content for particular J^{PC} . First we note that the lightest state, with no phonons at all, has $J = 0$. For this state the only action of both \mathcal{C} and \mathcal{P} is to exchange L with R . Thus we have $J^{PC} = 0^{++}$ and 0^{--} as degenerate ground states for $SU(N \geq 3)$ and just the 0^+ for $SU(2)$. This is precisely as observed - except for the $C = \pm$ degeneracy, which is a problem that we have already remarked upon. (Note that despite the splitting, the lightest two states in the spectrum are the 0^{++} and 0^{--} .) Continuing with the $C = +$ sector we observe, using eqn(3) and the fact that $m = 1$ phonons do not exist, that the lightest 2^{++} has $n_{m=2}^+ = 1$, the 0^{-+} has $n_{m=4}^+ = 1$ and $n_{m=2}^- = 2$, the 4^{++} has $n_{m=2}^+ = 2$ or $n_{m=4}^+ = 1$, the 1^{++} has $n_{m=3}^+ = 1$, $n_{m=2}^- = 1$, and the 3^{++} has $n_{m=3}^+ = 1$. Using eqn(6), and parity doubling for $J \neq 0$, this implies the following level ordering:

$$m_{0^{++}} < m_{2^{\pm\pm}} < m_{3^{\pm\pm}} < m_{4^{\pm\pm}} < m_{1^{\pm\pm}} \ll m_{0^{-+}} \quad : \text{model.} \quad (10)$$

There is a similar ordering for the $C = -$ states, with the 0^{--} as the lightest state.

In the lattice calculations of [3], the level ordering found is claimed to be

$$m_{0^{++}} < m_{2^{\pm\pm}} < m_{0^{-+}} < m_{1^{\pm\pm}} \quad : \text{lattice} \quad (11)$$

which accords with eqn(10) except that the 0^{-+} is slightly lighter than the 1^{++} , rather than being considerably heavier (by three phonon units). This discrepancy actually highlights an important question about the lattice calculations. In practice these use glueball operators that transform according to representations of the symmetry group of a square (or cube in three space dimensions). These do not distinguish between $J = 1$ and $J = 3$ or between $J = 0$ and $J = 4$. Conventionally one labels the state by the lowest J that can contribute on the assumption that this will be the lightest state. As we see here, within the flux tube model at any rate, this is not the case for either of these pairs of states. So is it possible that the lattice states have been mislabelled: that what has been called the 0^{-+} is actually the 4^{-+} and the $J = 1$ is actually $J = 3$? This question has been addressed in [3], where it was shown that the ‘smeared’ operators that are used, will typically have a (much) larger overlap onto the state of smallest J . This argument is only qualitative however, and where the state with larger J is *much* lighter, as occurs in the flux tube model with the 4^{-+} and 0^{-+} , a real question mark remains. This is something we shall return to below, when we perform a detailed numerical comparison between the (extended) flux tube model and the lattice spectrum. It is also something that has motivated us to try and develop lattice operators that approximate, for example, $J = 4$. Preliminary calculations of this kind [14] do indeed suggest that the 4^{-+} glueball has a mass that is close to that of the supposed 0^{-+} and a more definitive lattice study is currently under way [15].

2.2.2 semi-quantitative analysis

Using the above phonon content of the different glueball states, we can be a little more quantitative about the various masses. We begin with the lightest 0^{++} which possesses no phonons. So the mass will be dominated by the energy of the string, $2\pi\rho$. Since the theory has one mass scale, $\sqrt{\sigma}$, let us assume the string radius to be $1/\sqrt{\sigma}$. There is then the relatively small correction from the string Casimir energy, and a contribution from the kinetic term which will be smaller still if we assume $\frac{d^2}{d\xi^2}$ to be $\sim \sigma^{3/2}$. If we put all this into eqns(7,9), while neglecting the small kinetic contribution and ignoring the minor effect of the ‘fudge’ factor in eqn(8), we obtain the very rough estimate $m_{0^{++}} = m_{0^{--}} \sim 5\sqrt{\sigma}$. For comparison we note that $m_{0^{+}} \simeq 4.7\sqrt{\sigma}$ in SU(2) while for $SU(N \geq 3)$ $m_{0^{++}} \sim 4.2\sqrt{\sigma}$ and $m_{0^{--}} \sim 6.2\sqrt{\sigma}$. Good agreement for such a crude estimate. (Our guess for the the radius was, after all, quite arbitrary; we could have equally well chosen the diameter to be $1/\sqrt{\sigma}!$)

It is interesting to note that the model provides a natural explanation for the fact that the scalar glueball is lighter in $D=3+1$ than in $D=2+1$. In three space dimensions there are two directions transverse to the string, and so the Casimir energy is doubled. Using $\rho \sim 1/\sqrt{\sigma}$ as above, this tells us that $m_{0^{++}}/\sqrt{\sigma}$ should be lower by ~ 1 in $D=3+1$ than in $D = 2 + 1$. This is about right [3, 1].

The 2^{++} differs from the 0^{++} by possessing an $m = 2$ phonon. Thus we expect $m_{2^{++}} \simeq m_{0^{++}} + 2/\rho \simeq m_{0^{++}} + 2\sqrt{\sigma}$ and a similar relation between the 2^{--} and 0^{--} . This works quite well [3]:

$$\frac{m_{2^{++}}}{\sqrt{\sigma}} \simeq \frac{m_{0^{++}}}{\sqrt{\sigma}} + \begin{cases} 2 & : \text{model} \\ 3 & : \text{lattice} \end{cases} \quad (12)$$

$$\frac{m_{2^{--}}}{\sqrt{\sigma}} \simeq \frac{m_{0^{--}}}{\sqrt{\sigma}} + \begin{cases} 2 & : \text{model} \\ 2 & : \text{lattice} \end{cases} \quad (13)$$

A more reliable way to estimate how much a unit phonon increases the mass is to use the observed $J = 0, 2$ splittings, i.e. $(m_{2^{++}} - m_{0^{++}})/2 \simeq 1.5\sqrt{\sigma}$ and $(m_{2^{--}} - m_{0^{--}})/2 \simeq 1.0\sqrt{\sigma}$ for the $C = \pm$ sectors respectively. Using this we obtain the following naive model estimates to be compared with the lattice results:

$$\frac{m_{J^{++}}}{\sqrt{\sigma}} \simeq \frac{m_{0^{++}}}{\sqrt{\sigma}} + \begin{cases} 4.5 & : J = 3 \text{ model} \\ 7.5 & : J = 1 \text{ model} \\ 6.2 & : J = 1 \text{ lattice} \end{cases} \quad (14)$$

$$\frac{m_{J^{--}}}{\sqrt{\sigma}} \simeq \frac{m_{0^{--}}}{\sqrt{\sigma}} + \begin{cases} 3.0 & : J = 3 \text{ model} \\ 5.0 & : J = 1 \text{ model} \\ 3.7 & : J = 1 \text{ lattice} \end{cases} \quad (15)$$

and

$$\frac{m_{J^{-+}}}{\sqrt{\sigma}} \simeq \frac{m_{0^{++}}}{\sqrt{\sigma}} + \begin{cases} 6 & : J = 4 \text{ model} \\ 12 & : J = 0 \text{ model} \\ 5 & : J = 0 \text{ lattice} \end{cases} \quad (16)$$

$$\frac{m_{J^{++}}}{\sqrt{\sigma}} \simeq \frac{m_{0^{--}}}{\sqrt{\sigma}} + \begin{cases} 4 & : J = 4 \text{ model} \\ 8 & : J = 0 \text{ model} \\ 4 & : J = 0 \text{ lattice} \end{cases} \quad (17)$$

where we have deliberately paired the $J = 0, 4$ and $J = 1, 3$ model predictions because of the ambiguity in the lattice assignments. We observe that at this semi-quantitative level the flux tube model works remarkably well; particularly so if the lattice spin assignments in the ambiguous cases turn out to have been mistaken.

So far we have discussed only the lightest states in each J^{PC} sector. There will be further states due both to radial excitations and/or to extra phonons. We observe that because of the lack of $m = 1$ phonons, the first 0^{++} excitation due to phonons would require $n_{m=2}^+ = 1, n_{m=2}^- = 1$. This is rather heavy and it is therefore almost certain that the first one or two excited 0^{++} states will be radial excitations. The same remark can be made about the 2^{++} excitation, (although not, for example, about the 1^{++}). The model predicts widespread degeneracies amongst states of the same spin and of different spins. For example the lightest 4^{++} is degenerate, since one can form it from a phonon content of $n_{m=2}^+ = 2$ or $n_{m=4}^+ = 1$; and these will be degenerate with the excited 0^{++} formed with $n_{m=2}^+ = 1$ and $n_{m=2}^- = 1$. With a modest improvement in the lattice calculations one would be able to search for the lightest such (near-)degeneracies, which are a robust prediction of the assumption that the phonon dynamics is ‘fast’.

2.2.3 numerical solution

As we have seen, one can deduce many features of the predicted spectrum with almost no calculation, using what is essentially a classical approximation. This does not of course replace a full calculation of the spectrum of the quantised flux tube model; to which we now turn.

The mass spectrum of the flux tube model as specified in eqns(3-9), has been previously calculated in [7] and we shall now discuss some of the results from that (unpublished) paper. We begin with the model with no short-distance ‘fudge factor’; that is to say we set $F(\rho) = 1$ in eqn(7). Since σ only serves to set the overall mass scale, the predictions of this model for the masses, $m_G/\sqrt{\sigma}$, involve no parameters. In Tables 2 and 3 we show the lowest predicted masses in the different J^{PC} sectors, and we compare them with the lattice $SU(N \rightarrow \infty)$ values from Table 1.

Given that the model has no free parameters at all (and one should add that it was formulated at a time when nothing was known about the $D=2+1$ spectrum) the overall agreement is quite remarkable. In the $C=+$ sector it predicts a 0^{++} that is somewhat lighter than the actual value but, since this state will be the most sensitive to the inevitable breakdown of the simple flux tube picture at small radii, some mismatch here is no surprise. Otherwise the $C=+$ agreement is very good. Apart, that is, from the 0^{-+} . We have already noted that this discrepancy is a robust one. The $0^{-+}/0^{++}$ splitting involves 8 ($=4+2+2$) phonon units while the $2^{++}/0^{++}$ splitting involves 2 phonon units; it is simply not possible to lower the predicted 0^{-+} mass sufficiently to

agree with the lattice value, without getting the 2^{++} far too light. However we also note that the predicted 4^{-+} mass is close to the lattice 0^{-+} mass. And, as we have emphasised already, it might be that the lattice state whose mass has been calculated is actually the 4^{-+} and not the 0^{-+} . So for the moment it is not clear if this should be regarded as a failure or as a success of the model. In the $C = -$ sector the agreement is clearly worse, although the predicted level ordering is correct. (The same comments apply to the 0^{+-} as to the 0^{-+} .) The major discrepancy between the model and the actual spectrum is that the $C = \pm$ degeneracy predicted by the former is quite strongly broken in the latter.

One can ask what happens if we introduce a non-trivial $F(\rho)$ into the model, as in eqns(7,8). The answer may be found in Fig.1 and Fig.2 of [7] (although the lattice masses shown there should be replaced by the $SU(\infty)$ values in our Table 1). We note that the spectrum is not particularly sensitive to the cut-off parameter f , unless that is made unreasonably small. One can lift the predicted 0^{++} towards the lattice value, although at the cost of a worsening prediction for the 2^{++} . A choice of $f \simeq 3$ would seem to provide the most acceptable $C = +$ spectrum. It is however clear that the $C = -$ predictions cannot be improved upon in this way. Clearly we need to reconsider the model.

3 Generalising the Isgur-Paton flux tube model

In this section we point to several ways in which the original Isgur-Paton model can be generalised. We start with the observation that one can build on other strings than the fundamental. We then point out that a curvature term in the effective string action makes an important difference. The argument for both these extensions is compelling. We then turn to the short-distance fudge factor $F(\rho)$ in eqn(8), point out its shortcomings and suggest some alternatives. We leave to the next section the important question of how to split the $C = \pm$ spectra in a way that is both natural in terms of the string model and reproduces the main features of the observed splitting.

3.1 Extra strings, extra states

The flux tube in the Isgur-Paton model contains flux in the fundamental representation; it joins charges that are in that representation. For $SU(N \geq 4)$ there exist charges in higher representations which cannot be screened by virtual adjoint charges (i.e. gluons) down to the fundamental. One can label charges in these representations by the way they transform under a centre gauge transformation, $z \in Z_N$. If they acquire a factor z^k we will refer to them as having N -ality k . Since gluons transform trivially under the centre they cannot screen the N -ality of a charge. For each such charge we have a flux tube of a corresponding N -ality k , which will possess a string tension σ_k . We can consider a closed tube of such flux, and we can then build a whole spectrum of

glueball states on this flux string just as we did for the fundamental, $k = 1$, string in the Isgur-Paton model. Thus as N grows the spectrum will acquire extra towers of states that are identical to the spectrum obtained with the fundamental flux loop except that their overall energy scale is $\sqrt{\sigma_k/\sigma_1}$ (ignoring any mixing).

If observed, such a spectrum would be a remarkable manifestation of the underlying string structure of glueballs. Of course it is not guaranteed that such a spectrum actually exists in the string picture: this will depend on the dynamics. Consider for example the case of $SU(4)$. If it happens to be the case that $\sigma_{k=2} \not\propto 2\sigma_{k=1}$ then the $k = 2$ flux tube can break up into two $k = 1$ (fundamental) flux loops, so that the $k = 2$ states are just multi-glueball scattering states formed out of the $k = 1$ glueball states. In the $D = 3 + 1$ $SU(4)$ gauge theory it is now known [17] that $\sigma_{k=2} \simeq 1.4\sigma_{k=1}$ so the corresponding extra states should exist there. This result is compatible with the SUSY prediction [16] that $\sigma_k \propto \sin(\pi k/N)$. However corresponding calculations do not exist in $D = 2 + 1$ and the lattice calculations have not identified enough excitations (in each J^{PC} sector) to test for the possible presence of such extra states. We will therefore ignore this potential state replication in the remainder of this paper, apart from pointing to its great interest for future calculations.

3.2 Curvature/elasticity

The flux tube must have a finite thickness if it is to have a finite energy density; presumably it will be $O(1/\sqrt{\sigma})$. Such a finite flux tube will presumably possess an effective elasticity. Continuing in the language of classical mechanics, we recall that the free energy per unit length of a rigid bent rod is $\frac{1}{2}\mathcal{Y}\frac{1}{\rho^2}I$, where \mathcal{Y} is the Young's modulus and I is the moment of inertia perpendicular to the axis of bending. We expect \mathcal{Y} and I to be constant along the flux tube, thus integrating along the length of the flux tube

$$\oint \frac{1}{2}\mathcal{Y}I\frac{1}{\rho^2}dl \propto \frac{1}{\rho} \quad (18)$$

In string language this is a curvature term. For a meson, the curvature of the straight string joining the quarks is zero and so a curvature term would have no effect to the order in $1/\rho$ that we are including. For a closed string, on the other hand, the curvature is constant and integrates to a $\sim 1/\rho$ contribution as in eqn(18). The constant of proportionality, our effective elasticity, we denote by γ_E and we will regard it as an unknown free parameter. Note that we may regard the Casimir energy of the closed loop as simply renormalizing the elasticity

$$\gamma = \gamma_E - \frac{13}{12} \quad (19)$$

just as the $c\rho$ piece in eqn(5) was absorbed into a renormalisation of σ . Although there has been some discussion [18] as to the sign such an elasticity should take, we shall leave γ as a free parameter, whose value is to be determined by fitting to the spectrum.

3.3 Modification at short distances

Since the flux tube has a finite width, a glueball will presumably cease to look like an excited closed string when ρ is much less than that width. This is embodied in the Isgur-Paton model by a fudge-factor $F(\rho) = 1 - e^{-f\rho}$ which suppresses the contribution of the string phonons as $\rho \rightarrow 0$, as in eqns(7,8). The detailed form of $F(\rho)$ is largely arbitrary. As is the choice to suppress the phonon excitations but not the $2\pi\rho$ string contribution. Since the spectrum of the string model is non-singular when we set $F(\rho) = 1$, the effects of the suppression factor are not large and the details do not matter greatly. We have calculated the spectrum for various possibilities and we find that as far as the $C = +$ spectrum is concerned what one needs is a modest short-distance suppression so as to get the $0^{++}, 2^{++}$ splitting about right, and then one can tune the γ/ρ contribution so as to raise the overall spectrum to about the right level. That is to say one can easily get the 0^{++} and 2^{++} right, the 4^{-+} to be close to the lattice ' 0^{-+} ' and the 3^{++} and 1^{++} to straddle the lattice ' 1^{++} '.

A quite different possibility is to make the string tension a function of ρ rather than to impose a fudge-factor $F(\rho)$. This is motivated by a recent study [19] of closed flux tubes in the dual Ginzburg-Landau theory. They find that the effective string tension, $\sigma_{\text{eff}}(\rho)$, varies with ρ so as to vanish as $\rho \rightarrow 0$. One can in fact parameterise the observed variation quite accurately using

$$\sigma_{\text{eff}}(\rho) = \sigma(1 - e^{-1.72\rho}). \quad (20)$$

One can then quantise the string model with this ρ -dependent string tension and solve for its spectrum. Since $\sigma_{\text{eff}}(\rho)$ appears in the mass and hence in the kinetic energy of the loop, the quantisation is not entirely straightforward and we leave its description to the Appendix. (More details may be found in [10].) The qualitative effect of using a variable $\sigma_{\text{eff}}(\rho)$ in eqn(9) is that at small ρ the kinetic energy is enhanced relative to the potential energy. This is much the same as the effect of our fudge-factor $F(\rho)$. However it has the advantage that there is no free parameter (or functional form) to choose and there is no ambiguity as to how one should apply it.

Later on in this paper we will see how both of the above approaches work when confronted with the observed spectrum.

4 Splitting $C = +$ from $C = -$

We now turn to the problem of how one might split the $C = \pm$ spectra in a way that is both natural in terms of the string model and reproduces the main features of the observed splitting. We shall begin by summarising what these features are and we shall then consider a number of possible dynamical mechanisms. In each case we shall ask how well the main observed features are reproduced.

4.1 The observed $C = +/ -$ splitting

From the masses listed in Table 1 we see that the $C = +/ -$ splitting possesses the following qualitative features.

- In Fig.1 we plot two examples of the $C = \pm$ splitting, as a function of $1/N^2$. This is a natural variable to use since the leading corrections to the large- N limit are expected to be $O(1/N^2)$ [13]. We infer from this plot (and from similar plots of other states) that the splitting remains non-zero in the $N = \infty$ limit; it is a leading order effect.
- In $SU(2)$ there is no $C = -$ sector and one can ask what the $SU(2)$ 0^+ mass continues to as N increases. This will clearly depend on the dynamics that produces the $C = \pm$ splitting for $N \geq 3$. For example, if this dynamics simply splits the 0^{++} and 0^{--} equally from their naive degenerate masses, then we would expect the $SU(2)$ 0^+ to continue smoothly to the average of the 0^{++} and 0^{--} masses. As another example, if the shift involves just the 0^{--} , then the $SU(2)$ 0^+ will continue smoothly to the $N \geq 3$ 0^{++} . Conversely, if the shift affects just the 0^{++} , then the continuation should be with the 0^{--} . In Fig.2 we plot the 0^{++} and 0^{--} masses, as well as the average of the two, as a function of $1/N^2$. We see that in all cases the variation with N for $N \geq 3$ can be described using just a leading $\propto 1/N^2$ correction. We also note that the $SU(2)$ 0^+ mass extrapolates precisely from the 0^{++} masses while it is inconsistent with a smooth extrapolation of the averaged $C = \pm$ states or of the 0^{--} . The same is true for the tensor: the $SU(2)$ 2^+ mass is a smooth continuation of the $SU(N \geq 3)$ $2^{\pm+}$ masses, and not of the average of the $2^{\pm+}$ and $2^{\pm-}$ masses, or of the 2^{--} . We shall see that this observation provides a tough constraint on possible mechanisms for splitting the $C = +$ and $C = -$ sectors.
- The $C = \pm$ splitting appears to decrease as the mass increases. To be more specific we infer from

$$m_{0--} - m_{0++} > m_{0---*} - m_{0+++*}. \quad (21)$$

that states with larger radial quantum number, n_R , are split less than those with smaller n_R . (Recall that in the flux tube model these lowest excitations are radial rather than phonon.) Furthermore we infer from

$$\begin{aligned} m_{0--} - m_{0++} &= 1.85(26)\sqrt{\sigma} > m_{2--} - m_{2++} = 1.01(38)\sqrt{\sigma} \\ &> m_{1--} - m_{1++} = -0.62(65)\sqrt{\sigma} \end{aligned} \quad (22)$$

(obtained at $N = \infty$) that the magnitude of the splitting also decreases with increasing phonon number. (Recall that for the lightest $J = 0, 2, 1$ glueball states the total phonon number in eqn(4) is $M = 0, 2, 5$ respectively.) Note that the decrease we see is even faster when the splitting is expressed in terms of the average mass. All this provides constraints on possible splitting mechanisms.

In addition to the above there is another striking feature as emphasised in [3]: the spectrum seems to possess some intriguing approximate degeneracies between $C = +$

and $C = -$ states. In particular we note from Table 1 that

$$m_{0--} \simeq m_{0++*} \quad ; \quad m_{0---} \simeq m_{0++**} \quad ; \quad m_{2--} \sim m_{2-+*} \quad \dots \quad (23)$$

(although the last relation is more visible in SU(3) than at larger N). It might be that these apparent degeneracies are merely accidental. If not then it is tempting to generalise and infer that any excited $C = +$ state will be degenerate with the previous excitation in the corresponding tower of $C = -$ states. This possibility has provoked a recent suggestion [20] that what we are seeing is the $C = \pm$ degeneracy predicted by the Isgur-Paton model and that the very lowest mass states are produced by some other dynamics. One can motivate this on the grounds that the lightest states have the smallest size and hence are the least stringlike. This is a possible, even attractive, scenario but if it were the case it is not clear that it would make much sense to perform a detailed comparison with other parts of the low-lying spectrum, as we do here, since these states are not significantly larger. So in this paper we shall make the economical assumption that the model should be confronted with *all* the observed states, and we shall ignore the possibility that there is some quite different dynamics that might either remove or add some states to the spectrum. To explore this intriguing possibility will clearly require lattice calculations that are both more accurate and which include more excited states.

4.2 Direct mixing

Since a flux loop has a direction, L or R , it is convenient to introduce 2-component wave-functions:

$$\Psi \equiv \begin{pmatrix} \psi_L \\ \psi_R \end{pmatrix}. \quad (24)$$

In this notation, we can write $C = \pm$ states as

$$\Psi_{C=+} = \psi \begin{pmatrix} 1 \\ 0 \end{pmatrix} + \psi \begin{pmatrix} 0 \\ 1 \end{pmatrix} \quad ; \quad \Psi_{C=-} = \psi \begin{pmatrix} 1 \\ 0 \end{pmatrix} - \psi \begin{pmatrix} 0 \\ 1 \end{pmatrix} \quad (25)$$

and eqn(9) becomes

$$H_{IP} \Psi = \begin{bmatrix} H_L & 0 \\ 0 & H_R \end{bmatrix} \begin{pmatrix} \psi_L \\ \psi_R \end{pmatrix} = E \Psi \quad (26)$$

where $H_L \equiv H_R$ is the operator on the LHS of eqn(9).

With the above Hamiltonian there is no mixing between L and R states and hence no $C = \pm$ splitting. To obtain such a splitting we need a non-zero probability for a L state to turn into an R state and vice-versa i.e

$$\begin{pmatrix} \psi_L^\dagger & 0 \end{pmatrix} e^{-iHt} \begin{pmatrix} 0 \\ \psi_R \end{pmatrix} \neq 0. \quad (27)$$

which clearly requires some off-diagonal terms to appear in the Hamiltonian H . So we alter eqn(26) to define our ‘direct mixing’ Hamiltonian as

$$H_{dir}\Psi = \begin{bmatrix} H_L & \alpha \\ \alpha & H_R \end{bmatrix} \begin{pmatrix} \psi_L \\ \psi_R \end{pmatrix} = E\Psi \quad (28)$$

where we shall choose to keep α real.

We need to make some choice for α , and we will be motivated by the following simple physical picture that arises naturally in the flux tube model. For the lightest states the radius of the closed flux loop will not be much larger than the intrinsic width of the flux tube. Now when we quantise, the wavefunction will give some probability for loops of both smaller and larger radii. When the radius is smaller than the flux tube width, we have something that is no longer a distinct loop, but is rather some kind of ‘ball’ – which will no longer have any definite orientation. In a path integral picture, we can think of a path where a loop of orientation L (for example) shrinks into a ball, at which point it loses any memory of the initial orientation, and then expands into a loop that can be L or R with equal probability. This will lead to a finite transition amplitude between L and R loops.

In the above picture the mixing will be rapidly suppressed as ρ becomes larger than the flux tube radius and a well defined loop appears. Now we recall that in the Isgur-Paton model we suppressed, at short distances, the $O(1/\rho)$ contribution in eqn(9) for much the same reason. So it makes sense to use the same suppression factor, $F(\rho)$, as used there. That is to say, we choose

$$\alpha(\rho) = \alpha_0 \{1 - F(\rho)\} \quad (29)$$

where $F(\rho)$ is defined in eqn(7). This introduces one new parameter α_0 to be determined by fitting the spectrum.

We shall return later to ask how well this model fits the spectrum. For now we concentrate on its qualitative predictions. For that it suffices to make the approximation $H_L = H_R = M$ where M is a mass, and to replace $\alpha(\rho)$ by α_{eff} . Then the energy eigenstates are clearly

$$M_{C=\pm} = M \pm \alpha_{eff} \quad (30)$$

so that $C = \pm$ states are split equally from their common Isgur-Paton value. Three immediate predictions follow from the above.

- 1) Since α_{eff} decreases with increasing ρ we expect that states with larger radial quantum number, n_R , should be split less than those with smaller n_R . This qualitative expectation is indeed borne out as we saw in eqn(21).
- 2) On the other hand for states that are approximately of the same ρ , the splitting will be roughly the same independent of the phonon number. This should be the case, for example, for the lightest $J = 0, 1, 2$ states. However, as we have seen in eqn(22), the splitting does in fact vary a great deal amongst these states.

3) It is the average of the $C = +$ and $C = -$ masses that equals the mass with no mixing. As we decrease N from $N = \infty$ it is this average that should extrapolate to the $SU(N = 2)$ value of the 0^+ mass, because the Hamiltonian there is the same as H_L or H_R . (All this up to $O(1/N^2)$ corrections.) However we have seen in Section 4.1 that this is not the case: the $SU(2)$ 0^+ mass equals the $SU(N \geq 3)$ 0^{++} mass up to $O(1/N^2)$ corrections.

4) We expect the wavefunction to have a smooth limit as $N \rightarrow \infty$, and so the probability for ρ to be less than the flux tube radius should also have a non-zero limit. Thus the $L \leftrightarrow R$ mixing and the consequent $C = \pm$ splitting should be non-zero at $N = \infty$, just as is observed. (This appears to contradict the conventional statement [13] that mixings vanish as $N \rightarrow \infty$ but we believe that the standard arguments do not apply to our kind of ‘mixing’.)

A simple solution to the problem raised in the second of the above points is to make the mixing parameter α , which appears in eqn(29), a function of the total phonon number M . A suppression of α with increasing M is perhaps not entirely artificial: the presence of fluctuations on the string will prevent the radial distance $\rho(\phi)$ from becoming small for all angles and hence might well suppress the amplitude for the string to collapse into a ‘ball’.

To incorporate this dynamics into our mixing model we can replace $\alpha(\rho)$ in H_{dir} , as defined in eqn(28), by $\bar{\alpha}(\rho, M)$ where, for example, one might choose

$$\bar{\alpha}(\rho, M) = -\alpha(\rho)e^{-\zeta/\alpha M}. \quad (31)$$

This gives us another parameter ζ to fit to the spectrum and, not surprisingly, it can be chosen so as to reproduce much of the observed variation of the $C = \pm$ splitting with M . However if the $J = 1$ splitting is indeed negative, as it appears to be albeit within large errors, then this is something we cannot easily accommodate in this way.

Moreover, however we tune the parameters in this model, it remains the case that it is the average of the 0^{++} and 0^{--} masses that is predicted to continue smoothly to the $SU(2)$ 0^+ mass, and, as we have seen, this is contradicted by the lattice calculations. So other, perhaps less straightforward, mechanisms need to be considered.

4.3 Indirect mixing

We shall begin our discussion within $SU(3)$ because the mechanism we are going to introduce is easier to picture there.

In $SU(3)$ three fundamental charges can make a colour singlet and, similarly, three fundamental colour strings can end at a vertex, which we shall refer to as a Y vertex. (The colour indices at the vertex are knitted together by an ϵ_{ijk} .) A quantum fluctuation involving such vertices can interpolate between L and R flux loops as shown in Fig.3. This is clearly a ‘large’ quantum fluctuation and we do not know how to calculate the amplitude for this process. For the purposes of our calculation we shall assume

that the circle + diameter flux loop that occurs at the mid-point of our fluctuation represents a separate state that we shall refer to as a Y state. We will refer to it as ‘indirect’ mixing in contrast to the ‘direct’ mixing of the previous subsection.

Compared to the circular flux loop such a state has an extra energy $\Delta E \sim 2\sigma\rho + 2v_Y$ associated with the diameter and the two vertices. Thus it will be ‘heavy’ and we shall ignore its possible explicit presence in the spectrum. Indeed it might well be that there is in reality no such state. One may regard it as a simple device for keeping correct track of the quantum number flow in the process shown in Fig.3. The magnitude of the mixing will in any case be determined by fitting a free parameter.

The qualitative new feature of this approach arises from the fact that Ψ_Y has specific C quantum numbers. First we note that this loop is not rotationally invariant, and so we can build states of various J from it. (In contrast to our simple circular loops where any non-zero J had to be provided by phonons.) Second, applying C reverses all the arrows on the lines, and this is clearly equivalent to a rotation by π . So a $C = -$ projection of Y will flip sign under a rotation of π : i.e. it must have odd J . Similarly a $C = +$ projection of Y has even J .

Thus for $J = 0, 2, \dots$ this state will have $C = +$ and so will only mix with the low-lying $C = +$ states: the masses of the $C = -$ states will retain the values they possess in the simple Isgur-Paton model. For $J = 1, 3, \dots$ it is the $C = -$ states that are shifted and the $C = +$ states that are unchanged.

Clearly it will be convenient in this model to represent the wave-functions using 3 components. Furthermore, since the Y state has definite C quantum numbers, it will also be convenient to use a $\psi_{C=\pm} \sim \psi_L \pm \psi_R$ basis for our circular loops. We can then write

$$\Psi = \begin{pmatrix} \psi_+ \\ \psi_- \\ \psi_Y \end{pmatrix} \quad (32)$$

We have a corresponding matrix Hamiltonian

$$H_{indir} = \begin{bmatrix} H_+ & 0 & \alpha_{+Y} \\ 0 & H_- & \alpha_{-Y} \\ \alpha_{+Y} & \alpha_{-Y} & H_Y \end{bmatrix} \quad (33)$$

using an obvious notation. Of course $H_+ = H_- = H_L = H_R$; the subscripts are to remind us which objects they act on. We choose the mixing parameter to be real and to satisfy

$$\alpha_{+Y} = \alpha, \quad \alpha_{-Y} = 0 \quad J = 0, 2, \dots \quad (34)$$

$$\alpha_{-Y} = \alpha, \quad \alpha_{+Y} = 0 \quad J = 1, 3, \dots \quad (35)$$

so as to accord with the quantum numbers of the Y state.

To calculate the spectrum we need some ansatz for H_Y . How detailed we make this ansatz depends on how seriously we take the notion of a state obtained by quantising

our Y loop. At the moment we are only interested in the qualitative features of the spectrum so we make the simple approximation $H_+ = H_- = M$ and $H_Y = M_Y$. For any given value of J the mixing is actually two body, so the calculation is simple and we obtain for the splitting

$$M_{C=-} - M_{C=+} \simeq (-1)^J \frac{\alpha^2}{M_Y - M} \quad \text{for } 4\alpha^2 \ll (M_Y - M)^2 \quad (36)$$

where, if we neglect fluctuations, the energy of our basic circle+diameter Y loop will be

$$M_Y = 2\pi\sigma\rho + 2\sigma\rho + 2v \quad (37)$$

where v is some vertex energy. (See e.g. [21] for a discussion of its possible value.)

The above discussion has been for $SU(3)$, but it can easily be extended to $SU(N)$. Now the vertex v will have N fundamental strings ending on it, the diameter will consist of $N - 2$ coalesced strings and the energy will grow

$$E_Y = 2\pi\sigma\rho + 2\sigma_{N-2}\rho + 2v \propto N\sigma\rho \quad (38)$$

as N grows. If we insert this into eqn(36) we see that for low-lying states the splitting disappears

$$M_{C=+} - M_{C=-} \propto \frac{\alpha^2}{\sigma} \frac{1}{N} \quad (39)$$

for large N . This decrease will be accentuated by the inevitable mixing of the Y state with an increasing number of excited fundamental string states as M_Y increases, and also by the decreasing overlap of the wavefunctions (which appears in the explicit expression for α in terms of α_Y).

We can now list some of this model's qualitative features.

- 1) As we have just seen, we expect the $C = \pm$ splitting to vanish as $N \rightarrow \infty$. This contradicts what one observes and so would suggest that this mechanism can be at best a higher order correction to the main splitting mechanism.
- 2) Consider the lightest states for each J . For $J = 0$ and 2 it is the 0^{++} and 2^{++} that will mix with the ' Y ' state and this will shift their masses downwards. The 0^{--} and 2^{--} do not mix and their masses are unaffected. For $J = 1$ it is the 1^{--} that mixes and not the 1^{++} . So we find

$$m_{0^{++}} < m_{0^{--}} ; \quad m_{2^{++}} < m_{2^{--}} ; \quad m_{1^{--}} < m_{1^{++}} \quad (40)$$

This is consistent with the observed pattern, and it is particularly interesting that it naturally reproduces the apparent sign change in the splitting between even and odd spin states.

- 3) On the other hand this form of mixing would naively suggest that it is the unshifted 0^{--} for $N \geq 3$ that will smoothly continue to the 0^+ in $SU(2)$, since no analogue of

these ‘Y’ fluctuations exists there. This again is inconsistent with what one observes in practice.

A potential solution to point (1) is as follows. The $N - 2$ string introduced above has the same quantum numbers as a string of N -ality $k = 2$ (see Section 3.1). If we construct the Y loop using for the diameter such a $k = 2$ string instead of the $k = N - 2$ string that we have been using so far, then we would expect the energy E_Y to remain finite as $N \rightarrow \infty$. Of course this requires that $\sigma(k = 2) < 2\sigma(k = 1)$ since otherwise our Y loop simply falls apart into two fundamental loops; the Y state is then a mere scattering state of glueballs built on the fundamental flux loop. A sufficiently small value for $\sigma(k = 2)$ has been shown to occur in various D=3+1 MQCD theories where one finds [16] that

$$\frac{\sigma(k)}{\sigma(1)} = \frac{\sin(\frac{\pi k}{N})}{\sin(\frac{\pi}{N})} \quad (41)$$

and it has been conjectured [16] that eqn(41) also holds in $SU(N)$ gauge theories. That $\sigma(k = 2) < 2\sigma(k = 1)$ in D=3+1 $SU(4)$ gauge theories has been suggested some time ago by the lattice calculations of [24] and more recent calculations in [17] provide much more detailed evidence for the approximate validity of eqn(41). So it is amusing to note that if we were to assume that this D=3+1 (M)QCD prediction were to hold for D=2+1, then for $N = 3$ we would have $\sigma(k = 2) = \sigma(k = 1)$ i.e. the $SU(N > 3)$ Y state based on a $k = 2$ diameter smoothly continues down to the $SU(3)$ Y state considered in this Section. Of course, intriguing as these possibilities may be, they must be considered speculative until there is some explicit confirmation that $\sigma(k = 2) < 2\sigma(k = 1)$ in D=2+1.

As for point (3), one might try to imagine an analogue of the ‘ Y ’ state whose quantum numbers would be $C = -$ for $J = 0$ so that the 0^{++} remains unshifted and continues down to the $SU(2)$ 0^+ . But we have failed to construct such a fluctuation within the class of models that can be considered at all natural. We turn now to a more successful idea.

4.4 Adjoint string mixing

We pointed out in Section 3.1 that in $SU(N \geq 4)$ theories there exist extra strings and hence extra states. Since these are just scaled up versions of our fundamental string spectrum they would not help in splitting $C = +$ from $C = -$. However there is another type of string in the theory that we have not yet considered: the one that carries adjoint flux. Such a string carries no arrow: it is intrinsically $C = +$. So any mixing would affect the $C = +$ spectrum: the 0^{++} mass would (probably) be driven down while the 0^{--} would be left undisturbed. But this does not lead to problems with the 0^+ in $SU(2)$ because the same adjoint string exists in $SU(2)$ and would drive down the 0^+ mass there as well. So we have a mechanism that might at last explain why the $SU(2)$ 0^+ smoothly interpolates onto the 0^{++} for $SU(N > 2)$.

The problem with this mechanism is, of course, that the adjoint string can be broken by gluon pair production so it is not clear if it makes sense to use a closed adjoint loop as the basis for a set of states. However we know that as $N \rightarrow \infty$ the string becomes stable [13] so at least for large N it can be used in this way. Since, as we have seen, lattice studies [3] find that the low-lying $SU(2)$ spectrum differs only by small corrections from $SU(N = \infty)$, it is reasonable to assume that the adjoint string has developed only a modest decay width in $SU(2)$. (As indeed seems to be the case [23] in 3+1 dimensions.) If so then the decay time will be long compared to the characteristic time scale of the low-lying string modes, and we can safely quantise the string in the Isgur-Paton fashion; the only extra feature being that these states will have finite but small decay widths (at least for the lowest masses). We will assume that this is so from now on, although an explicit lattice verification would clearly be very helpful.

We can use exactly the same formalism as in the previous subsection defining

$$\Psi = \begin{pmatrix} \psi_+ \\ \psi_- \\ \psi_a \end{pmatrix}. \quad (42)$$

However since ψ_a always has $C = +$, the Hamiltonian

$$H_{adj} = \begin{bmatrix} H_+ & 0 & \alpha_a \\ 0 & H_- & 0 \\ \alpha_a & 0 & H_a \end{bmatrix} \quad (43)$$

is quite simple: we can clearly reduce it to a two-component calculation in the $C = +$ sector, and a simple Isgur-Paton calculation in the $C = -$ sector. We shall assume that there is no mixing between fundamental and adjoint loop states that have differing phonon occupation numbers.

In eqn(43) $H_+ = H_-$ is the usual Isgur-Paton Hamiltonian. H_a will be identical except that the scale is set by the adjoint string tension, σ_a , rather than by the fundamental σ . It is frequently speculated that σ_a and σ are related by the ratio of quadratic Casimirs

$$\frac{\sigma_a}{\sigma} = \frac{2N^2}{N^2 - 1}. \quad (44)$$

Lattice calculations in $D = 2+1$ [22] find that for $SU(2)$ $\sigma_a \simeq 2.5\sigma$, which is quite close to the value of $8/3$ one obtains from eqn(44). Thus we expect the spectrum of states based on the adjoint loop to be quite massive. Indeed, if we assume a simple two body mixing, with H_+ replaced by $M = m_{0--}$ and H_a by $M_a \simeq 1.5M$, and if we choose α so as to obtain the observed m_{0++} mass, we find that the lightest scalar ‘adjoint’ state has $M_{a,0++} \simeq 1.8m_{0--}$. This is light enough to be important by its explicit presence in the spectrum, in addition to affecting the fundamental states through mixing.

How can the fundamental flux loop mix with an adjoint loop? Once again our underlying physical picture is that for small ρ all these loops become ‘balls’ that are

no different from each other. Thus $\alpha(\rho)$ should peak at low ρ as in eqn(29). We now have the qualitative predictions:

- 1) As with the direct mixing of Section 4.2, we expect the mixing, and hence the splitting, to be leading order in N , as is observed.
- 2) As remarked above, since the adjoint loop mixes with just the $C = +$ sector and does so for all $SU(N \geq 2)$ gauge theories, we expect the $SU(2)$ 0^+ mass to continue smoothly on to the $SU(N > 2)$ 0^{++} masses, as is observed.
- 3) Since $\alpha(\rho)$ is peaked at small ρ , we expect larger, heavier states to show less splitting – as observed.
- 4) Whether the splitting decreases with increasing phonon number M at fixed radial number n_R is however not clear – it requires a detailed calculation.

The observed pattern of the $C = \pm$ splitting has proved very constraining on possible dynamics, but the model in which the fundamental loop mixes with an adjoint loop appears to have the right qualitative features. In the next section we shall see how well it can do at the quantitative level.

5 Fitting the lattice spectrum

We saw in the previous section that we can reproduce most of the qualitative features of the observed $C = \pm$ splitting if we suppose that the states built on the loop of fundamental flux mix with states built on a loop of adjoint flux. Since the latter states are all $C = +$ we have a simple picture in which the $C = -$ states are just as in the naive Isgur-Paton model, while the $C = +$ states are shifted from their naive values by mixing with this new sector of states.

In Section 4.4 we estimated the effects of this mixing by approximating the entries in the Hamiltonian by just the lightest masses – as we did earlier in eqn(30) and in eqn(36). In the present case (and indeed in the latter case as well) this is an uncontrolled approximation for the following reason. The lightest 0^{++} state formed from an adjoint loop is about 50% more massive than the lightest 0^{++} formed from the fundamental loop and will thus be closer in mass to some of the excitations of the latter. In this case a two-state mixing approximation has no justification. To do better we return to H_{adj} in eqn(43)

$$\Psi = \begin{pmatrix} \psi_+ \\ \psi_a \end{pmatrix} \quad ; \quad H_{adj} = \begin{bmatrix} H_+ & \alpha_a \\ \alpha_a & H_a \end{bmatrix} \quad (45)$$

truncated (with no loss of generality) to the $C = +$ basis. Let us represent H_{adj} as a large matrix, \hat{H} , in a basis given by the energy eigenstates of H_+ and of H_a . Suppose the energy eigenvalues and eigenstates of H_+ are $\{E_{f,i}, \psi_{f,i}; i = 1, \dots, n_f\}$ and of H_a are

$\{E_{a,i}, \psi_{a,i}; i = 1, \dots, n_a\}$. Then the Hermitian matrix \tilde{H} has diagonal entries

$$\tilde{H}_{ii} = \begin{cases} E_{f,i} & i \leq n_f \\ E_{a,i-n_f} & i > n_f \end{cases} \quad (46)$$

and off-diagonal matrix elements given by

$$\tilde{H}_{ij} \equiv \alpha_{ij} = \int D\rho \psi_{f,i}^\dagger(\rho) \alpha_a(\rho) \psi_{a,j-n_f}(\rho) \quad i \leq n_f ; j > n_f \quad (47)$$

and $\tilde{H}_{ij} = 0$ otherwise. The eigenvalues of this large non-diagonal matrix are the masses of the spectrum. The eigenfunctions of the matrix will be vectors \vec{v}_I and the corresponding eigenfunctions of the original Hamiltonian, H_{adj} , will be

$$\Psi = \begin{pmatrix} \sum_{i=1}^{n_f} v_i \psi_{f,i} \\ \sum_{i=1}^{n_a} v_{i+n_f} \psi_{a,i} \end{pmatrix} \quad (48)$$

Now, the larger are the energy differences $|E_{f,i} - E_{a,j}|$ and the smaller are the off-diagonal elements $\int D\rho \psi_{f,i}^\dagger(\rho) \alpha_a(\rho) \psi_{a,j}(\rho)$ the smaller will be the splitting of these masses from the original unmixed masses. We are interested in the lowest 2 or 3 masses for each J and in this case the nearest adjoint loop states are about 50% heavier (because $\sigma_a \geq 2\sigma$). In addition higher excitations will have more nodes in their wavefunctions so typically α_{ij} will be quite small except for the mixing of fundamental and adjoint ground states. Thus in our case it should be sufficient to include in the analysis just the lowest one, or possibly two, adjoint loop states.

In practice we do not use the above formalism to determine the mass spectrum, but rather we solve directly the pair of coupled differential equations represented by $H_{adj}\Psi = E\Psi$. (As described in the Appendix.) However when we want to identify the nature of any given low-lying state, then this formalism provides the tools to do so. Solving these equations, and their ‘direct mixing’ analogue, we shall see how well a generalised flux tube model can reproduce the lattice mass spectrum. But first we must discuss, in the next subsection, what we mean by fitting the lattice spectrum.

5.1 The data to be fitted

The generalised flux tube model typically has two or three unknown parameters. First there is γ , the (renormalised) curvature/elasticity. Secondly there is the mixing parameter characterised by a strength α_0 and with a weighting to small ρ characterised by f . The same f will typically characterise the short-distance cut-off imposed in the Isgur-Paton model. Alternatively we can use $\sigma_{eff}(\rho)$ instead of σ at short distances and this enables us to do without the parameter f . We can then solve the model for various values of these parameters and find which fits the lattice spectrum the best.

There are however some problems with just taking the mass spectrum as given in Table 1 and doing a least- χ^2 fit on the model parameters. First we have already seen

that the model prediction is always going to be far from the lattice 0^{-+} , so including it in the fit might badly distort the final ‘best fit’. Moreover there are theoretical reasons for thinking that the lattice 0^{-+} spin assignment might be mistaken and that this is actually a 4^{-+} . (And, similarly, that the lattice 0^{+-} is really a 4^{+-} .) To a lesser extent similar questions arise with the purported $J = 1$ states. We shall therefore exclude these states from the fit but will instead quote the values for these masses, as predicted by the best fit to the other states.

A second problem is that the most accurate masses are for the lightest states. Having the smallest errors these will provide the most important component of the χ^2 function that determines the best fit. On the other hand the lightest states possess the smallest radius ρ and so we expect the flux loop model to suffer the largest corrections for such states. Thus we might not want them to dominate, and so possibly distort, the best fit.

This second problem has no unambiguous resolution. The fact is that we know that the model is a simple approximation that can at best incorporate only the essential features of glueball structure. The most that we can expect is that it roughly reproduces the spectrum and whether it can do so is what we want to learn when we fit the model to the data. To do this we need to embody what we mean by ‘roughly’ in some specific way into the fitting procedure. The way we choose to do this is to give the masses an extra error that is 5% of the mass, and add it in quadrature with the statistical error. (For a more sophisticated Bayesian version of this see [10].) That is to say, we are saying that we want to know if the model can fit the masses within $\pm 5\%$. Of course the best fit might do better than that; but at least it will not be driven by the very small errors on the lightest masses for which it is probably least reliable.

5.2 Fitting the lattice spectrum

We have performed a large variety of comparisons with the lattice spectrum. We have used all the different $C = \pm$ splitting mechanisms described in this paper; we have fitted to all the lattice masses or just to a more reliable subset as discussed above; we have used the actual errors in the χ^2 or expanded errors as described above; we have used explicit short distance fudge factors of various kinds or a ρ -dependent string tension as described earlier, or indeed no suppression at all. The reader will be relieved to learn that we do not intend to describe this very large number of model fits here but will rather focus on two of the most relevant examples. Some different model fits can be found in [9] and others will appear in [10].

In this section we will describe what we find when we fit the lattice data with adjoint string mixing, as described in Section 4.4, or with direct mixing, as described in Section 4.2. In both cases we shall use a ρ -dependent string tension, as described in Section 3.3, to embody the short distance corrections to the flux tube picture, in a way that introduces no new parameters. In our physical picture of the mixing, we see

it as occurring at small ρ and so we choose the mixing term in eqns(28, 43) to satisfy

$$\alpha(\rho) = \alpha \left(1 - \frac{\sigma_{eff}(\rho)}{\sigma_{eff}(\infty)} \right) \quad (49)$$

(where we now drop the subscript on α_a). In the case of adjoint mixing we determine the adjoint string tension from eqn(44). Thus there are two parameters to be fitted: $\gamma = \gamma_E - 13/12$, where γ_E is the string curvature described in Section 3.2, and α , the mixing strength.

In each case we obtain the predicted spectrum by solving the coupled set of differential equations using the numerical technique described in the Appendix. We then scan through the parameter space to find the best χ^2 fit. (With just two parameters such a crude approach works reasonably well.) In order not to be unduly biased by the very small errors on the lightest masses, we have enhanced the errors by 5%, as described in Section 5.1. (In practice the best fits turn out to be similar whether we perform such an enhancement or not.) The best fit is determined using the lightest three states in each of the 0^{++} and 0^{--} sectors and the lightest two in the $2^{\pm+}$ and $2^{\pm-}$ sectors.

We do not show fits using the ‘indirect mixing’ mechanism described in Section 4.3 because it fails on too many grounds to make it an attractive candidate on its own. For example it naturally predicts a $C = \pm$ splitting that vanishes as $N \rightarrow \infty$. And it predicts that the $SU(2)$ 0^+ mass should be a continuation of the 0^{--} mass for $SU(N \geq 3)$. Moreover the detailed calculation invariably produces a 1^{--} state that is much too light. (This is the lightest ‘Y’ state in the $C = -$ sector which is clearly odd under rotations of π and so has $J = 1$.) As we remarked in Section 4.3 some of these problems might be solved by using a string of N -ality two for the diameter in Fig.3; but only if such a double string forms a bound state; as it is known to do in four dimensions [17, 24]. Until lattice calculations show that such bound states of strings also exist in three dimensions, any such discussion must remain speculative.

In Table 4 we list the mass spectra that one obtains from the best fits to the various $SU(N)$ spectra displayed in Table 1, in the case where we use the adjoint mixing mechanism. The corresponding results for the direct mixing mechanism are listed in Table 5. We have remarked that there are reasons to think that these simple models should work best in the $N \rightarrow \infty$ limit, and so we compare in Table 6 the results of the best direct mixing model fit to the extrapolated lattice spectrum. Table 7 does the same for the adjoint mixing model. The parameters corresponding to all these fits are listed in Table 8 and Table 9. In these Tables we also show χ_5^2 , the total χ^2 with a 5% error enhancement, as well as χ_0^2 , the value with no error enhancement. In calculating these values of χ^2 we have assumed that the lattice 0^{-+} and 0^{+-} states are in fact 4^{-+} and 4^{+-} . As we have pointed out, this is a quite reasonable possibility. If however this assumption turns out to be incorrect then the resulting discrepancy will be so large, and its origins will be so robust and simple, that the credibility of the model would be seriously damaged. There is a similar ambiguity with the $J = 1$ and $J = 3$ states but here any mis-labelling makes much less difference and so we ignore it.

We see from the Tables that the best fits, whether obtained using the direct or the adjoint mixing mechanisms, are, overall, of reasonable quality. As expected, and as we see from Tables 9 and 4, the parameters of the adjoint mixing interpolate quite smoothly through all values of N , albeit within large errors. More specifically this is also true of the predicted lightest 0^{++} mass, as can be seen in Table 4. Amusingly, the parameters of the direct mixing best fits are also consistent with being smooth in N ; however this is partly because the model is poor at reproducing the N -dependence of the lightest 0^{++} , as we see from Table 5. We also note that the adjoint mixing model does better as N increases, which supports our general theoretical expectation.

A closer examination of the detailed spectra does however show that both models have some real difficulties. In particular, the adjoint mixing is clearly unable to reproduce anything close to a large enough $0^{++}/0^{--}$ splitting. The direct mixing does much better on this, but only at the cost of being very poor on the $0^{++}/0^{++*}/0^{++**}$ splittings. The essential problem here is that the observed $0^{++}/0^{++*}$ splitting is too small for the generic flux tube model; it would prefer the 0^{++*} to be closer to the observed mass of the 0^{++**} . The way that the adjoint mixing model avoids this problem is that the mass of the lightest adjoint loop state is naturally close to that of the 0^{++*} , because $\sqrt{\sigma_a/\sigma_f} \sim 1.5$. Thus, after mixing, the 0^{++*} can be largely an adjoint loop, and the 0^{++**} can then be (largely) the first fundamental loop excitation. This suggests that a flux tube model that combines both direct and adjoint mixing should be able to do much better than either model alone. Combining these models is quite natural; our picture for the way an oriented fundamental loop may evolve into an adjoint loop (through contracting into a small ‘disoriented’ ball) is precisely the way we saw the direct mixing between fundamental loops of opposite orientation proceeding. This picture will, in general, require two mixing parameters. While it is interesting to explore these ideas [10] the analysis would clearly benefit from improved lattice calculations where a larger number of excited states are accurately determined.

Returning to the best fit parameters listed in Tables 9 and 4, we observe that all our fits require γ to be quite close to zero. Taken together with eqn(19) this tells us that the observed mass spectra do indeed require a non-zero curvature (elasticity) term, $\gamma_E \in [0.5, 1.0]$, in the effective string model for the confining flux tube.

Finally we remark that the features we have described are not only robust against the detailed fitting procedures used but much the same conclusions are obtained if we replace the ρ dependence of the string tension with a short distance modification of the kind shown in eqns(7,8).

6 Conclusions

In this paper we set out to test the idea that glueballs are quantised closed strings of colour-electric flux. Such a picture arises naturally in linearly confining theories, such as $SU(N)$ gauge theories in 2+1 and 3+1 dimensions, where distant fundamental

charges are connected by flux tubes.

We started out with the specific dynamical framework of the Isgur-Paton flux tube model [6], in which the excitations of the closed flux loop are either radial or phonon-like, and we confronted its mass spectrum with the rather accurate mass spectra available in D=2+1 SU(N) gauge theories [3]. As $N \rightarrow \infty$ the gauge theory simplifies in ways which bring it closer to some of the model's assumptions, e.g. the neglect of decays, and so one can argue that a comparison in this limit makes particular sense. If we express the observed masses in units of the observed string tension, then the model's predictions for these dimensionless ratios involve no free parameters at all. We found that these predictions were, for the most part, quite remarkably good in the $C = +$ sector of states; and for the $C = -$ sector they embodied the main qualitative features even if the quantitative comparison was less good.

Of course, when the flux tube radius, ρ , is smaller than the flux tube width the picture must break down and this is usually embodied in the model by suppressing the potential energy below $\rho \sim 1/f$, where f is a parameter that needs to be determined but which we expect to be $O(\sqrt{\sigma})$. In this paper we described other ways of including such a cut-off; in particular through a dependence of the string tension on ρ . By taking $\sigma(\rho)$ from calculations in the literature [19], one can avoid having the additional parameter f to fit. We then pointed out that one should in general include a string curvature term, which for a closed loop will make a contribution γ_E/ρ to the effective potential that is of the same form as the Casimir string energy. This introduces a parameter γ that needs to be determined. Finally we noted that the $C = \pm$ degeneracy in the model mass spectrum is contradicted by the splittings seen in the lattice spectrum and we were compelled to consider dynamical mechanisms that might reproduce these splittings. Such mechanisms typically involve a mixing parameter α that also needs to be determined.

The qualitative features of the observed $C = \pm$ splittings proved to be very constraining. The only mechanism that we were able to construct that was natural, simple and had the right qualitative behaviour, involved adding to the basic flux tube model a sector of states built on closed loops of adjoint flux. These are intrinsically $C = +$ and we introduced a mixing between these states and the $C = +$ states built on the fundamental loop. We pictured the mixing as arising at small ρ where a closed flux tube becomes a flux-less 'ball', and we conjectured that this kind of mixing may be leading order in $1/N$, as required by the lattice spectrum. However when we performed detailed numerical calculations of the mass spectrum of this extended model, we found that it could not, in practice, reproduce the full magnitude of the observed $C = \pm$ splitting in the scalar sector. The implication of these calculations and also calculations with other mixing mechanisms, such as a direct mixing between fundamental loops of opposite orientation, was that the simultaneous presence of adjoint loop and direct mixing was likely to be much more successful in quantitatively reproducing the observed spectrum.

In searching for the best fit to the observed spectrum, we found that whatever mixing mechanism we used we invariably required a substantial string curvature contribution, $\gamma_E \in [0.5, 1]$.

However even these best fits always left us with one very large discrepancy (in addition to having some trouble with the size of the observed $0^{++}/0^{--}$ splitting). This one prominent discrepancy concerned the 0^{-+} state. In the model this is a highly excited state (involving eight phonon units) and is predicted to be much heavier than the lattice 0^{-+} . This is a robust result of the model: the splitting of the 0^{++} and 2^{++} states, which is two phonon units, is what essentially determines the 0^{-+} mass. On the other hand the predicted 4^{-+} mass is very close to the lattice 0^{-+} mass. This suggests that the lattice calculation may have mislabelled this state; after all one cannot distinguish $J = 0$ from $J = 4$ by the rotational symmetries of a square lattice. This has provoked lattice calculations that are attempting to resolve this rather basic question [14, 15].

If there are states built on the adjoint loop they will be about half as heavy again as the corresponding states built on the fundamental loop and so only the very lightest are likely to be present in the currently available lattice spectrum. Moreover, since the adjoint loop can break, these states may have large decay widths, their masses may be shifted from their naive values, and perhaps only the lightest states will actually exist. However, with a modest improvement in the quality of the lattice calculations, one could search for their presence. The same improvement would allow us to search for degeneracies between states of differing J but with the same number of phonon ‘units’. For example there will be an excited 0^{++} with phonon content $n_{m=2}^+ = n_{m=2}^- = 1$ that should be degenerate with a 4^{++} with phonon content $n_{m=2}^+ = 2, n_{m=2}^- = 0$. Such (near) degeneracies provide a characteristic pattern that would test the general dynamics of the Isgur-Paton flux tube model.

In $SU(N \geq 4)$ gauge theories there are additional strings than the fundamental which will be stable if their string tensions are low enough. In D=3+1 this is expected to be the case on theoretical grounds [16], and indeed is known to be the case for $SU(4)$ [17, 24]. Thus the string model predicts that, if we neglect mixings and decays, the observed mass spectrum will contain towers of states that are exact scaled-up replicas of the spectrum arising from the fundamental string, and that the number of these ‘towers’ of states will grow as $N \rightarrow \infty$. This is a dramatic and robust prediction of the basic flux tube picture which can and needs to be investigated by lattice calculations.

We have seen that the kind of exercise undertaken in this paper, testing a model against lattice calculations, has a fruitful impact in both directions. We have been forced to generalise the model in ways that, in retrospect, are entirely natural. And the model points to both potential weaknesses in the lattice calculations and motivates specific further calculations that promise to be very informative however they turn out.

Acknowledgments

We are grateful to Jack Paton for valuable discussions during the course of this work. One of us (RWJ) would like to thank the Rhodes Trust for financial support.

Appendix

In this Appendix we shall begin by briefly recalling how one arrives at eqn(9). We then describe how we solve this equation numerically. Finally we discuss how we generalise the formalism to accommodate an effective string tension that varies with the loop radius.

1. The Isgur-Paton Hamiltonian

We have a circular loop of mass $\mu = 2\pi\rho$ which moves in an effective potential provided by the phonon modes etc. as discussed earlier in this paper. Thus the kinetic and potential terms are:

$$T = \frac{p_\rho^2}{4\pi\sigma\rho} \quad ; \quad V = 2\pi\sigma\rho + F(\rho)\frac{M + \gamma}{\rho}. \quad (50)$$

where $F(\rho)$ is the usual short distance fudge-factor, which we shall now set to unity for convenience. Under the transcription $p_\rho \rightarrow i\hbar\frac{\partial}{\partial\rho}$ we have (with $\hbar = 1$)

$$T = \frac{p_\rho^2}{2\mu} \rightarrow \frac{-1}{4\pi\sigma} \frac{\frac{\partial}{\partial\rho} \frac{\partial}{\partial\rho}}{\rho}. \quad (51)$$

We want canonical variables ξ, P_ξ such that T is quadratic in P_ξ . In passing from the above classical system to the quantum system there is an ambiguity how to order the various terms in T . We choose $P_\rho = \frac{\partial}{\rho^{\frac{1}{2}}}$ so that $T \propto P_\rho^2$. That is to say we choose

$$\xi = \rho^{\frac{3}{2}}, \quad (52)$$

so that

$$T \rightarrow \frac{-1}{4\pi\sigma} \left(\frac{3}{2}\right)^2 \frac{\partial^2}{\partial\xi^2} = \frac{-9}{16\pi\sigma} \frac{\partial^2}{\partial\xi^2} \quad (53)$$

and we arrive at eqn(9).

2. Numerical solution

Our approach to solving

$$\frac{-9}{16\pi\sigma} \frac{\partial^2}{\partial\xi^2} \psi + V(\rho(\xi))\psi = E\psi. \quad (54)$$

will closely follow [25]. First we transform variables from $\xi \in (0, \infty)$ to $t \equiv \frac{1}{1+\xi} \in (0, 1)$ and define $\Phi = t\psi$. Then eqn(54) becomes

$$\frac{\partial^2}{\partial t^2} \Phi + V' \frac{\Phi}{t^4} - E' \frac{\Phi}{t^4} = 0 \quad (55)$$

where $E' = E/(\frac{-9}{16\pi\sigma})$ and $V' = V/(\frac{-9}{16\pi\sigma})$.

We now discretise t

$$t_j = jh, \quad h = \frac{1}{n+1}, \quad j \in [0, n+1] \quad (56)$$

and define $\Phi(t) \rightarrow \Phi_j \equiv \Phi(t_j)$ with the boundary conditions $\Phi(0) = \Phi(1) = 0 \Rightarrow \Phi_0 = \Phi_{n+1} = 0$. We use the second order approximation

$$\frac{\partial^2}{\partial t^2} \Phi_j \approx \frac{1}{12h^2} (-\Phi_{j-2} + 16\Phi_{j-1} - 30\Phi_j + 16\Phi_{j+1} - \Phi_{j+2}), \quad (57)$$

which receives its first correction from the $h^6 \frac{\partial^6}{\partial t^6} \Phi$ term in the Taylor expansion around $\Phi(t = t_j)$. We thus obtain as our discretisation of eqn(54)

$$S\Phi \equiv S_b\Phi + \frac{12}{j^4h^2} [V' - E'] \Phi = 0. \quad (58)$$

where S_b (and S) are appropriate $n \times n$ matrices and Φ is to be thought of as a vector with components Φ_j ; $j = 1, \dots, n$. Because of eqn(57) S is in fact a band matrix with, in general, five non-zero elements centered on the diagonal. This is not possible for the first and last two rows of the matrix; we have to be more specific about the boundary conditions. We have already set $\Phi_0 = \Phi_{n+1} = 0$ so that leaves Φ_{-1} and Φ_{n+2} to be defined. Following [25], we set $\Phi_{n+2} = -\Phi_n$ and $\Phi_{-1} = \Phi_1$. The off-diagonal terms in the extreme rows of the matrix S will therefore be altered so as to embody eqn(57) with these boundary conditions.

To rewrite eqn(58) as a standard eigenproblem

$$A\mathbf{x} = E'\mathbf{x}, \quad (59)$$

we define a diagonal matrix K with $K_{jj} = j^2$ and rewrite eqn(58) as

$$KSK \left(K^{-1}\Phi \right) = 0 \quad (60)$$

so that we obtain the desired form of eqn(59) with

$$A - E' = \frac{h^2}{12} KSK = \frac{h^2}{12} j^4 S_b + V' - E' \quad (61)$$

The eigenvalues E'_I ; $I = 1, \dots, n$ and the corresponding (as yet un-normalised) eigenstates $\mathbf{x}_I = K^{-1}\Phi_I$ can now be obtained by standard numerical methods. We observe that

$$\sum_j x_j^2 = \sum_j \frac{1}{j^4} \Phi_j^2 \simeq h^3 \int_0^1 dt \frac{1}{t^4} \Phi^2(t) \quad (62)$$

gives us the measure in t . Thus choosing the normalisation $\sum x_j^2 = h^3$ will give us

$$\int dt \frac{1}{t^4} \Phi_I(t) \Phi_J(t) = \delta_{IJ} \quad (63)$$

which, recalling that $\Phi = t\psi$ and $t = 1/(1 + \xi)$, translates into

$$\int d\xi \psi_I(\xi) \psi_J(\xi) = \delta_{IJ}. \quad (64)$$

This defines for us the integration measure in terms of the wavefunctions appearing in the Isgur-Paton equation. It can be rewritten as an integral over ρ using eqn(52).

3. Generalising to $\sigma(\rho)$

If the vacuum of non-Abelian gauge theories is a (type-II) dual superconductor, then flux tubes will arise through a dual Meissner effect. Thus it is interesting and relevant to ask how closed flux tubes behave as the radius is varied in the Ginzburg-Landau theory of type-II superconductors. As pointed out in [19] what happens is that the effective string tension $\sigma_{\text{eff}}(\rho)$ vanishes as $\rho \rightarrow 0$, roughly as in eqn(20). If we replace σ in the Isgur-Paton model by such a $\sigma_{\text{eff}}(\rho)$ we will be providing the model with a short-distance cut-off that is both natural and employs no free parameters. The price for this is some complication in the quantisation of the model. However, as we shall now see, this is a problem that can be overcome.

As we saw earlier, the tricky term in quantizing the Isgur-Paton model is the kinetic energy, so that is where we will begin. Abusing notation slightly,

$$T = \frac{p_\rho^2}{2\mu} \rightarrow \frac{-1}{4\pi} \left(\frac{\frac{\partial}{\partial \rho}}{\sqrt{\sigma_{\text{eff}}(\rho)\rho}} \right)^2, \quad (65)$$

where $\sigma_{\text{eff}}(\rho)$ is now included in the ρ dependence of the kinetic energy. If σ_{eff} were a constant, we would get T as in eqn(53). Now we must find a canonical variable ξ such that

$$\frac{\frac{d\xi}{d\rho} \frac{d}{d\xi}}{\sqrt{\sigma_{\text{eff}}(\rho)\rho}} = \frac{d}{d\xi} \quad (66)$$

or

$$d\xi = \sigma_{\text{eff}}^{\frac{1}{2}}(\rho) \rho^{\frac{1}{2}} d\rho \quad (67)$$

Substituting the function in eqn(20) for σ_{eff} , we find

$$\xi = \sigma^{\frac{1}{2}} \int d\rho \rho^{\frac{1}{2}} (1 - e^{-1.72\rho})^{\frac{1}{2}}. \quad (68)$$

where the integration constant has been determined by the boundary condition $\xi(0) = 0$. This integral cannot be put into closed form, yet we need the inverse function explicitly so as to substitute it into the potential $V(\rho(\xi))$. While it would be nice to include explicitly the function from [19], any function which approximates it reasonably well will suffice. So rather than using eqn(20) we shall use a less natural form, but one that will suit our manipulations better. Now, we need a function for $\sigma_{\text{eff}}(\rho)$ which goes to zero as $\rho \rightarrow 0$ and which approaches σ as $\rho \rightarrow \infty$, and which is integrable with respect to the measure $\rho^{\frac{1}{2}} d\rho$. As an example consider

$$\sigma_{\text{eff}}(\rho) = \sigma \left(1 - e^{-f\rho^{\frac{3}{2}}}\right)^2 \quad (69)$$

which, with a suitable value for f , will crudely approximate the dependence found in [19]. Performing the integral, and imposing $\xi(0) = 0$, we have

$$\xi = \sigma^{\frac{1}{2}} \int d\rho \rho^{\frac{1}{2}} \left(1 - e^{-f\rho^{\frac{3}{2}}}\right) = \frac{2}{3} \sigma^{\frac{1}{2}} \left(\rho^{\frac{3}{2}} - \frac{1}{f} + \frac{1}{f} e^{-f\rho^{\frac{3}{2}}}\right). \quad (70)$$

We cannot find the functional inverse explicitly, but as we are ultimately working with a discrete set $\{\xi_j\}$ related to $\{t_j\}$, we can simply solve the equation numerically to give ρ_j which we can put into the potential $V = V(\rho(\xi_j))$. (In practice we have used $\sigma_{\text{eff}} = \sigma(1 - e^{-f\rho})^2$ which leads to a slightly more complex relation than the above.) Returning to the kinetic energy,

$$T \rightarrow \frac{-1}{4\pi} \frac{\partial^2}{\partial \xi^2}, \quad (71)$$

and we proceed with the numerical solution of the discretised equation as described earlier.

References

- [1] M. Teper, hep-th/9812187.
- [2] C. Morningstar and M. Peardon, Phys. Rev. D60 (1999) 034509 (hep-lat/9901004).
- [3] M. Teper, Phys. Rev. D59 (1999) 014512 (hep-lat/9804008).
- [4] T. H. Hansson, in *Non-perturbative Methods* (Ed. S.Narison, World Scientific 1985).
- [5] G. Karl and J. Paton, Phys. Rev. D61 (2000) 074002 (hep-ph/9910413).
- [6] N. Isgur and J. Paton, Phys. Rev. D31 (1985) 2910.
- [7] T. Moretto and M. Teper, hep-lat/9312035.
T. Moretto, D.Phil Thesis, Oxford University (1993).
- [8] V. Agostini, G. Carlino, M. Caselle, and M. Hasenbusch, Nucl. Phys. B484 (1997) 331 (hep-lat/9607029).
- [9] R. Johnson and M. Teper, Nucl. Phys. Proc. Suppl. 63 (1998) 197 (hep-lat/9709083).
- [10] R. Johnson, D. Phil Thesis, in preparation.
- [11] M. Lüscher, K. Symanzik and P. Weisz, Nucl. Phys. B173 (1980) 365.
- [12] Ph. de Forcrand, G. Schierholz, H. Schneider and M. Teper, Phys. Lett. 160B (1985) 137.
- [13] G. 't Hooft, Nucl. Phys. B72 (1974) 461.
E. Witten, Nucl. Phys. B160 (1979) 57.
S. Coleman, 1979 Erice Lectures.
A. Manohar, 1997 Les Houches Lectures, hep-ph/9802419.
- [14] R. Johnson and M. Teper, Nucl. Phys. Proc. Suppl. 73 (1999) 267 (hep-lat/9808012).
- [15] R. Johnson and M. Teper, in progress.
- [16] A. Hanany, M. Strassler and A. Zaffaroni, Nucl. Phys. B513 (1998) 87 (hep-th/9707244).
M. Strassler, Nucl. Phys. Proc. Suppl. 73 (1999) 120 (hep-lat/9810059).
- [17] B. Lucini and M. Teper, Oxford preprint OUTP-00-56P and work in progress.

- [18] H. Kleinert and A. M. Chervyakov, hep-th/9601030.
- [19] Y. Koma, H. Suganuma and H. Toki, Phys. Rev. D60 (1999) 074024 (hep-ph/9902441).
- [20] J. Paton, private communication.
- [21] A. Momen and C. Rosenzweig, Phys. Rev. D56 (1997) 1437.
- [22] G. Poulis and H. Trottier, Phys. Lett. B400 (1997) 358 (hep-lat/9504015).
P. Stephenson, Nucl. Phys. B550 (1999) 427 (hep-lat/9902002).
- [23] S. Deldar, Phys. Rev. D62 (2000) 034509 (hep-lat/9911008).
G. Bali, hep-lat/0006022.
- [24] M. Wingate and S. Ohta, hep-lat/0006016.
- [25] K. J. Miller and M. G. Olsson, Phys. Rev. D25 (1982) 2383.

state	SU(2)	SU(3)	SU(4)	SU(5)	$m_G/\sqrt{\sigma}$
0^{++}	4.718(43)	4.329(41)	4.236(50)	4.184(55)	4.065(55)
0^{++*}	6.83(10)	6.52(9)	6.38(13)	6.20(13)	6.18(13)
0^{++**}	8.15(15)	8.23(17)	8.05(22)	7.85(22)	7.99(22)
0^{--}		6.48(9)	6.271(95)	6.03(18)	5.91(25)
0^{--*}		8.15(16)	7.86(20)	7.87(25)	7.63(37)
0^{---*}		9.81(26)	9.21(30)	9.51(41)	8.96(65)
0^{-+}	9.95(32)	9.30(25)	9.31(28)	9.19(29)	9.02(30)
0^{+-}		10.52(28)	10.35(50)	9.43(75)	9.47(116)
2^{++}	7.82(14)	7.13(12)	7.15(13)	7.19(20)	6.88(16)
2^{++*}		—	8.51(20)	8.59(18)	—
2^{-+}	7.86(14)	7.36(11)	6.86(18)	7.18(16)	6.89(21)
2^{-+*}		8.80(20)	8.75(28)	8.67(24)	8.62(38)
2^{--}		8.75(17)	8.22(32)	8.24(21)	7.89(35)
2^{--*}		10.31(27)	9.91(41)	9.79(45)	9.46(66)
2^{+-}		8.38(21)	8.33(25)	8.02(40)	8.04(50)
2^{+-*}		10.51(30)	10.64(60)	9.97(55)	9.97(91)
1^{++}	10.42(34)	10.22(24)	9.91(36)	10.26(50)	9.98(25)
1^{-+}	11.13(42)	10.19(27)	10.85(55)	10.28(34)	10.06(40)
1^{--}		9.86(23)	9.50(35)	9.65(40)	9.36(60)
1^{+-}		10.41(36)	9.70(45)	9.93(44)	9.43(75)

Table 1: Glueball masses in units of the string tension; in the continuum limit [3]. The $SU(\infty)$ values are obtained by extrapolating the $SU(N \leq 5)$ values with an $O(1/N^2)$ correction.

$m_G/\sqrt{\sigma}$		
J^{PC}	SU(∞)	IP model
0 ⁺⁺	4.065(55)	3.12
0 ^{++*}	6.18(13)	6.46
0 ^{++**}	7.99(22)	8.72
2 ^{±+}	6.88(16)	6.79
2 ^{±+*}	8.62(38)	9.06
0 ⁻⁺	9.02(30)	13.86
4 ^{±+}	—	9.64
1 ^{±+}	10.00(25)	10.84
3 ^{±+}	—	8.30

Table 2: Glueball masses in units of the string tension. Predictions of the simple no-parameter Isgur-Paton flux tube model compared to the actual spectrum of the $SU(N = \infty)$ theory, in the $C = +$ sector.

$m_G/\sqrt{\sigma}$		
J^{PC}	SU(∞)	IP model
0 ⁻⁻	5.91(25)	3.12
0 ^{--*}	7.63(37)	6.46
0 ^{--**}	8.96(65)	8.72
2 ^{±-}	7.94(35)	6.79
2 ^{±-*}	9.62(66)	9.06
0 ⁺⁻	9.47(116)	13.86
4 ^{±-}	—	9.64
1 ^{±-}	9.38(60)	10.84
3 ^{±-}	—	8.30

Table 3: Glueball masses in units of the string tension. Predictions of the simple no-parameter Isgur-Paton flux tube model compared to the actual spectrum of the $SU(N = \infty)$ theory, in the $C = -$ sector.

state	$m_G/\sqrt{\sigma}$			
	SU(2)	SU(3)	SU(4)	SU(5)
0 ⁺⁺	4.82	4.28	4.12	4.17
0 ^{++*}	6.86	7.12	6.69	6.37
0 ^{++**}	8.19	8.81	8.39	8.14
0 ⁻⁻		5.21	4.99	4.86
0 ^{--*}		8.24	8.07	7.97
0 ^{--**}		10.21	10.02	9.92
0 ⁻⁺	14.06	14.13	14.00	13.93
0 ⁺⁻		14.21	14.07	13.98
4 ⁻⁺	9.99	9.89	9.75	9.72
4 ⁺⁻		10.21	10.02	9.92
2 ^{±+}	7.56	7.28	7.13	7.14
2 ^{±+*}	9.92	9.66	9.42	9.29
2 ^{±-}		7.84	7.63	7.52
2 ^{±-*}		10.24	10.08	9.99
1 ^{±+}	11.10	11.07	10.93	10.88
1 ^{±-}		11.29	11.12	11.02
3 ^{±+}	8.81	8.63	8.49	8.47
3 ^{±-}		9.05	8.86	8.75

Table 4: Best fit of the adjoint-mixing flux tube model to the $SU(N)$ glueball masses, in units of the string tension.

state	$m_G/\sqrt{\sigma}$			
	SU(2)	SU(3)	SU(4)	SU(5)
0 ⁺⁺	4.67	4.00	3.81	3.78
0 ^{++*}	7.84	7.54	7.38	7.35
0 ^{++**}	9.77	9.34	9.17	9.14
0 ⁻⁻		5.93	5.62	5.42
0 ^{--*}		8.60	8.38	8.25
0 ^{--**}		10.61	10.40	10.27
0 ⁻⁺	13.86	13.66	13.52	13.48
0 ⁺⁻		14.43	14.25	14.15
4 ⁻⁺	9.77	9.34	9.17	9.14
4 ⁺⁻		10.65	10.40	10.27
2 ^{±+}	7.35	6.80	6.61	6.59
2 ^{±**}	9.86	9.61	9.46	9.42
2 ^{±-}		8.42	8.14	7.98
2 ^{±**}		10.56	10.35	10.23
1 ^{±+}	10.88	10.51	10.35	10.32
1 ^{±-}		11.67	11.45	11.32
3 ^{±+}	8.59	8.10	7.92	7.89
3 ^{±-}		9.56	9.31	9.15

Table 5: Best fit of the direct-mixing flux tube model to the $SU(N)$ glueball masses, in units of the string tension.

$m_G/\sqrt{\sigma}$					
J^{PC}	$SU(\infty)$	model	J^{PC}	$SU(\infty)$	model
0 ⁺⁺	4.065(55)	3.72	0 ⁻⁻	5.91(25)	5.24
0 ^{++*}	6.18(13)	7.29	0 ^{--*}	7.63(37)	8.12
0 ^{++**}	7.99(22)	9.66	0 ^{--**}	8.96(65)	10.13
2 ^{±+}	6.88(16)	6.53	2 ^{±-}	7.94(35)	7.81
2 ^{±**}	8.62(38)	9.37	2 ^{±**}	9.62(66)	10.11
0 ⁻⁺	9.02(30)	13.43	0 ⁺⁻	9.47(116)	14.04
4 ^{±+}	-	9.08	4 ^{±-}	-	10.13
1 ^{±+}	10.00(25)	10.26	1 ^{±-}	9.38(60)	11.19
3 ^{±+}	-	7.84	3 ^{±-}	-	9.00

Table 6: Glueball masses in units of the string tension. Predictions of the direct-mixing flux tube model with mixing parameter $\alpha = -2.86$ and curvature $\gamma_E = \gamma + 13/12 = 0.54$. Compared to the observed spectrum of the $SU(N = \infty)$ theory.

$m_G/\sqrt{\sigma}$					
J^{PC}	SU(∞)	model	J^{PC}	SU(∞)	model
0 ⁺⁺	4.065(55)	4.02	0 ⁻⁻	5.91(25)	4.84
0 ^{++*}	6.18(13)	6.35	0 ^{--*}	7.63(37)	7.96
0 ^{++**}	7.99(22)	8.14	0 ^{--**}	8.96(65)	9.90
2 ⁺⁺	6.88(16)	7.03	2 ^{±-}	7.94(35)	7.50
2 ^{±*}	8.62(38)	9.20	2 ^{±**}	9.62(66)	9.98
0 ⁻⁺	9.02(30)	13.91	0 ⁺⁻	9.47(116)	13.97
4 ^{±+}	-	9.65	4 ^{±-}	-	9.90
1 ^{±+}	10.00(25)	10.83	1 ^{±-}	9.38(60)	11.01
3 ^{±+}	-	8.39	3 ^{±-}	-	8.73

Table 7: Glueball masses in units of the string tension. Predictions of the adjoint-mixing flux tube model with mixing parameter $\alpha = 4.14$ and curvature $\gamma_E = \gamma + 13/12 = 0.78$. Compared to the actual spectrum of the $SU(N = \infty)$ theory.

direct mixing				
group	α	γ	$\chi^2_0/\text{d.o.f}$	$\chi^2_5/\text{d.o.f}$
SU(2)	-	-0.42±0.12	46.5	4.7
SU(3)	-3.7±0.6	-0.18±0.10	31.8	3.1
SU(4)	-3.5±0.6	-0.37±0.10	23.4	3.6
SU(5)	-3.1±0.6	-0.45±0.10	18.8	3.4
SU(∞)	-2.9±0.6	-0.54±0.11	16.4	3.6

Table 8: Best fit parameters of the direct mixing model; α is the mixing strength and $\gamma = \gamma_E - 13/12$, where γ_E is the string curvature. The χ^2 per degree of freedom is shown. χ^2_0 uses the lattice statistical errors, while χ^2_5 adds to these errors that are 5% of the corresponding masses. The best fit used the latter errors.

adjoint loop mixing				
group	α	γ	$\chi_0^2/\text{d.o.f}$	$\chi_5^2/\text{d.o.f}$
SU(2)	2.2 ± 1.5	-0.19 ± 0.07	2.8	0.3
SU(3)	5.6 ± 1.0	-0.04 ± 0.09	28.6	2.9
SU(4)	4.7 ± 0.9	-0.20 ± 0.08	19.8	2.8
SU(5)	3.8 ± 0.8	-0.29 ± 0.08	7.3	1.9
SU(∞)	4.1 ± 0.8	-0.30 ± 0.08	4.4	1.7

Table 9: Best fit parameters of the adjoint mixing model; α is the mixing strength and $\gamma = \gamma_E - 13/12$, where γ_E is the string curvature. The χ^2 per degree of freedom is shown. χ_0^2 uses the lattice statistical errors, while χ_5^2 adds to these errors that are 5% of the corresponding masses. The best fit used the latter errors.

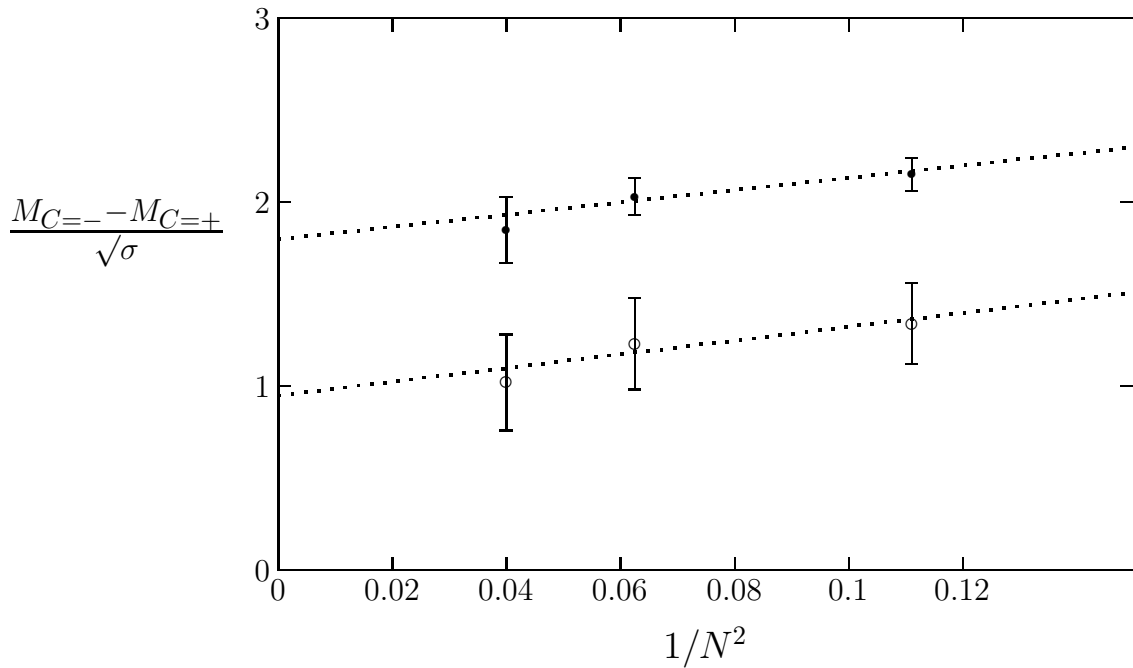


Figure 1: Some of the observed $SU(N)$ $C = \pm$ splittings plotted versus $1/N^2$: the mass difference between the 0^{--} and the 0^{++} (●) and that between the $2^{\pm-}$ and the $2^{\pm+}$ (○). As $N \rightarrow \infty$ the dependence is expected to be linear in $1/N^2$, i.e. like the straight lines added to the plot to guide the eye.

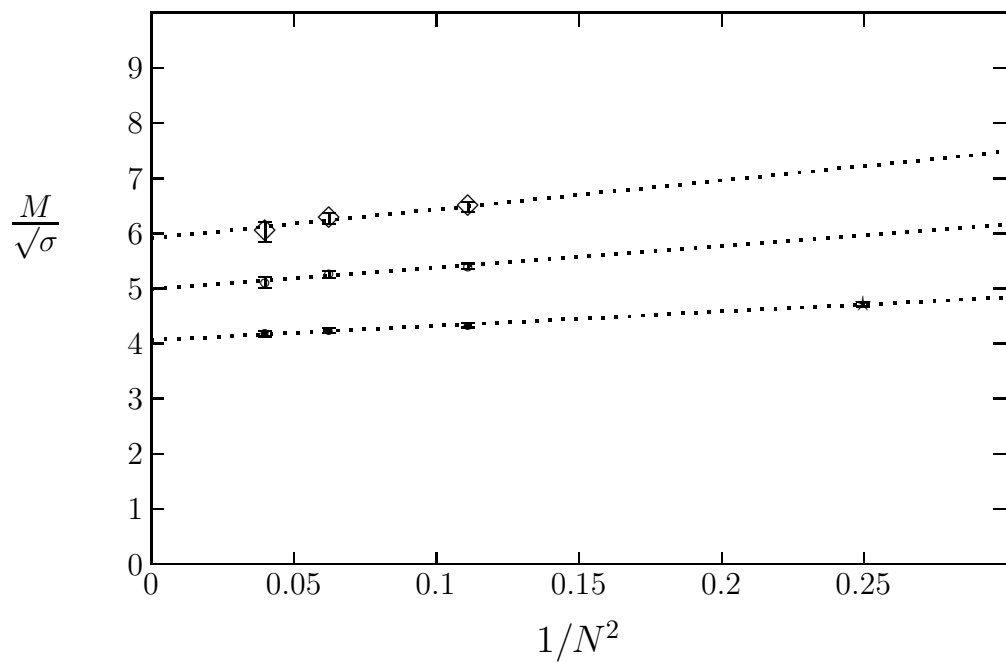


Figure 2: The $SU(2)$ 0^+ mass (\star), the $SU(N \geq 3)$ 0^{++} masses (\bullet), the $SU(N \geq 3)$ 0^{--} masses (\diamond), and the average of the 0^{++} and 0^{--} masses (\circ), plotted against $1/N^2$; with the expected large- N linear dependence shown in each case.

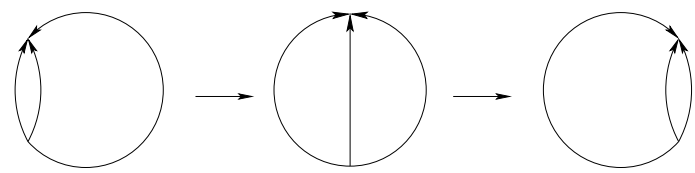


Figure 3: The Y mixing scenario for the case of $SU(3)$.